Journal of Industrial Microbiology & Biotechnology (2002) 29, 339–346

www.nature.com/jim

A mathematical model of quorum sensing in a growing bacterial biofilm

DL Chopp[1,a], MJ Kirisits[2,a], B Moran[2,3] and MR Parsek[2]

[1]*Department of Engineering Sciences and Applied Mathematics, Northwestern University, Evanston, IL 60208, USA;* [2]*Department of Civil and Environmental Engineering, Northwestern University, Evanston, IL 60208, USA;* [3]*Department of Mechanical Engineering, Northwestern University, Evanston, IL 60208, USA*

In a process called quorum sensing, bacteria monitor their population density *via* extracellular signaling molecules and modulate gene expression accordingly. This paper describes a one-dimensional model of a growing *Pseudomonas aeruginosa* biofilm. Quorum sensing has been included in the model by the addition of equations describing the production, degradation, and diffusion of acyl-homoserine lactones in the biofilm. In order for quorum sensing to initiate near the substratum, in accordance with experimental observations, model results suggest that cells in oxygen-deficient regions of the biofilm must still be synthesizing the signal compound. This result highlights the importance of careful study of the relationship between metabolic activity of the bacterium and signal synthesis.
Journal of Industrial Microbiology & Biotechnology (2002) **29,** 339–346 doi:10.1038/sj.jim.7000316

Keywords: acyl-homoserine lactone; biofilm; cell–cell signaling; *Pseudomonas aeruginosa*; quorum sensing; reaction–diffusion equation

Introduction

Bacteria have traditionally been viewed and studied as independent entities. However, it is becoming increasingly clear that many bacteria have the ability to monitor their own population density and modulate gene expression accordingly in a process called quorum sensing. Although there are a number of different mechanisms by which quorum sensing can function, perhaps the best-characterized quorum sensing mechanism is the acyl-homoserine lactone (acyl-HSL)-based system used by a number of Gram-negative bacteria [10,11]. The physiological processes regulated by quorum sensing in these different species vary from biofilm formation [6] to conjugal plasmid transfer [23].

The molecular scheme of acyl-HSL-based quorum sensing is relatively simple (Figure 1a). The bacterium produces an acyl-HSL synthase enzyme (LuxI-type protein), which catalyzes the synthesis of acyl-HSLs at a low basal rate [11]. As shown in Figure 1a, LasI is the enzyme that catalyzes synthesis of the 3-oxododecanoyl-homoserine lactone signal in *Pseudomonas aeruginosa* [18,19]. At low cell densities, the signal diffuses out of the cell, down its concentration gradient, and is lost to the environment. However, at high cell densities, the local concentration of acyl-HSL builds to the inducing concentration (critical threshold) at which it interacts with a transcriptional regulator (LuxR-type protein [10,11]). LasR is such a transcriptional regulator in *P. aeruginosa* [12] (Figure 1b). This acyl-HSL transcriptional regulator complex modulates expression of quorum sensing-regulated genes. In many cases, this involves positive autoregulation of the quorum sensing *luxI* and *luxR* homologs. In *P. aeruginosa*, there are two separate quorum sensing systems, *las* and *rhl*, and each system has its own signal synthase, transcriptional regulator, and specific acyl-HSL [20,21]. Quorum sensing in *P. aeruginosa* is also modulated by a quinolone-like signal, and evidence exists that signal production levels differ between planktonic and biofilm cells [22,29].

A limitation of our understanding of the acyl-HSL mechanism is that almost all of the studies have been conducted in liquid batch culture where the cells exist in a homogeneous environment. In the natural environment, bacteria predominantly form heterogeneous surface-attached communities called biofilms [32]. A biofilm can be defined as a microbial population attached to a surface and encased in a matrix of extracellular polymeric substances (EPS), primarily of biotic origin [4]. Besides being spatially fixed, biofilm bacteria have been shown to be physiologically distinct from free-swimming cells of the same species [24,26,33]. A hallmark characteristic of biofilms is that they are extremely resistant to antimicrobial stress [3,4,30]. Therefore, biofilms are difficult to eradicate and cause a variety of problems in clinical and industrial situations.

Another consequence of the biofilm lifestyle is the presence of chemical and nutrient gradients. Since bacteria at the periphery of a biofilm are exposed to higher nutrient concentrations, they are generally more metabolically active than bacteria buried deep within the biofilm [3,35]. A biofilm community will also presumably experience gradients of signaling molecules, as opposed to a shaken liquid culture where the signal concentration is uniform. How signal gradients affect patterns of signal response in a biofilm is unknown.

There are several important parameters of a biofilm that presumably will affect signal production. The concentration (vol/vol)

Correspondence: Dr Matthew R Parsek, Department of Civil and Environmental Engineering, Northwestern University, A312 Technological Institute, 2145 Sheridan Road, Evanston, IL 60208-3109, USA
[a]DL Chopp and MJ Kirisits contributed equally to this work.
Received 11 March 2002; accepted 1 August 2002

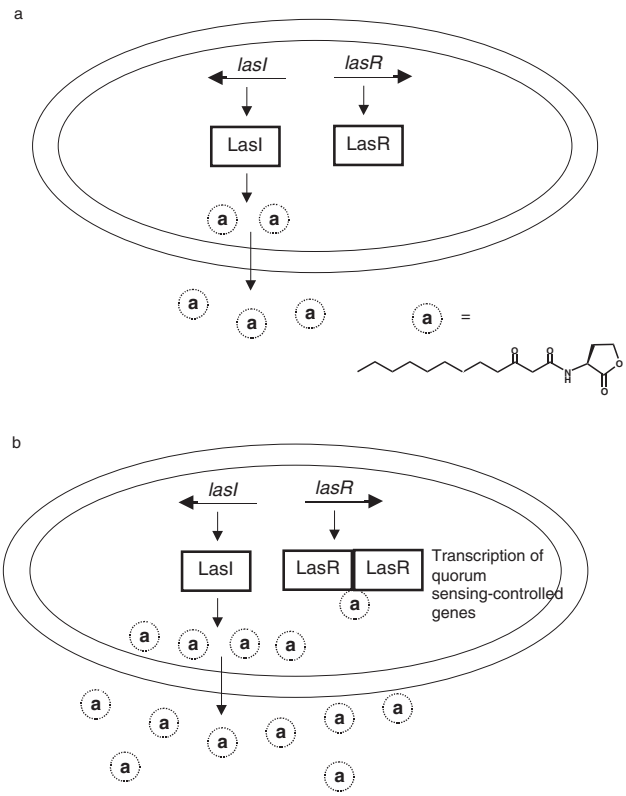

Figure 1 *lasI–lasR* quorum sensing in *P. aeruginosa*. (a) Low signal (3-oxododecanoyl-homoserine lactone) concentration at low cell density. (b) High signal concentration at high cell density causes induction of quorum sensing.

of active cells in the biofilm, which is affected by cell growth and death rates and the diversion of electrons for the production of EPS, will affect acyl-HSL production in a biofilm. Another factor to consider is the concentration of limiting growth substrates. As mentioned before, biofilm populations experience a gradient of physiological activity due to substrate availability. Heterogeneity in cell metabolic activity will likely affect the availability of cellular substrate pools for signal synthesis, *S*-adenosylmethionine, and acyl–acyl carrier protein, thereby affecting signal production [14,17,27].

Since these and other parameters have the potential to affect signaling in a biofilm, it is useful to describe this system mathematically. Such a mathematical model facilitates exploration of the relationship between various biofilm parameters and quorum sensing. Results from the mathematical model can be used to formulate significant research questions and to refine research direction. Conversely, properly designed research questions can help to refine the mathematical model.

The model presented in this paper describes a growing one-dimensional *P. aeruginosa* biofilm. The biofilm is separated into two compartments. The first compartment consists of active cells, and the second compartment contains inert biomass, EPS, and water. Net biofilm growth is a function of the diffusion of oxygen, which is the limiting substrate, and cell decay. Quorum sensing has been included in the model by the addition of equations describing the production, degradation, and diffusion of acyl-HSLs in the biofilm. To simplify the model, we have focused on only one of *P. aeruginosa*'s two quorum sensing systems, the *las* system. Also, for simplicity, we have chosen to assume that there is no significant difference in acyl-HSL production patterns between planktonic and biofilm cells.

Derivation of model equations

Table 1 names the variables and parameters used in this model.

Kinetics

We begin by addressing the kinetics of the system. Let f_x be the volume fraction of active biomass in a biofilm, and let f_w be the volume fraction of inactive material, including inert biomass, EPS, and water. The net production of active biomass is given by $\mu_x f_x \rho_x$ where:

$$\mu_x = Y_{x/o}\frac{\hat{q}_o o}{K_o + o} - b\frac{o}{K_o + o}. \quad (1)$$

In Eq. (1), the first term describes the synthesis of new biomass as a result of substrate consumption, and the second term describes the death of bacterial cells. Since oxygen was assumed to be the limiting substrate, Monod kinetics was used in Eq. (1).

The production of inactive material is given by $\mu_{wx} f_x \rho_x$ where:

$$\mu_{wx} = (1-f_D)b\frac{o}{K_o + o} + Y_{w/o}\frac{\hat{q}_o o}{K_o + o}. \quad (2)$$

Here, b is the same parameter that was used in Eq. (1), and it represents the death of active biomass. A fraction of dead cells cannot be biodegraded ($1-f_D$), and the first term in Eq. (2) therefore represents the accumulation of inert biomass (i.e., non-biodegradable dead cell material). The second term in Eq. (2) describes the production of EPS. Monod kinetics was used in Eq. (2) because oxygen was considered to be the limiting substrate for both processes.

Oxygen, the limiting substrate, is consumed at the rate $\mu_o f_x \rho_x$ where:

$$\mu_o = -(\hat{q}_o + \gamma f_D b)\frac{o}{K_o + o}. \quad (3)$$

In Eq. (3), the first term describes consumption of oxygen for synthesis of new cells. The second term accounts for the consumption of oxygen for degradation of the biodegradable fraction of the active biomass (f_D).

The signal compound (acyl-HSL) is produced by the active biomass at the rate $\mu_a f_x \rho_x$ where:

$$\mu_a = \frac{\beta_1 o}{K_o + o} + \beta_3 + \beta_2 H(a - a_0). \quad (4)$$

The first two terms in Eq. (4) represent the basal rate of signal production; this is the rate of signal production prior to the activation of quorum sensing. It is hypothesized that the rate of signal production partially depends on the metabolic state of the active biomass. In the first term of Eq. (4), a Monod term describes the metabolic state of the active biomass. If the biomass is located in a region of oxygen depletion, the first term in Eq. (4) will be small, and the basal synthesis rate will essentially be β_3. Conversely, if the biomass is located in an oxygen-rich region of the biofilm, then the basal signal synthesis rate will be elevated to $(\frac{\beta_1 o}{K_o + o} + \beta_3)$.

Table 1 Model variables and parameters

Name	Description	Value	Reference
f_x	Volume fraction of active biomass in the biofilm	$f_x(0,z)=0.8$	Estimated
f_w	Volume fraction of inactive material in the biofilm	$f_w(0,z)=0.2$	Estimated
ρ_x	Biomass density (mass of cell per volume of cell)	1.0250 mg VSS/mm^3	BE Rittmann[a]
ρ_w	Inactive material density	1.0125 mg VSS/mm^3	BE Rittmann[a]
o	Concentration of rate-limiting substrate, dissolved oxygen	$o(0,z)=8.3\times10^{-6}$ mg O_2/mm^3	NA
a	Concentration of signal compound, acyl-HSL	$a(0,z)=0$ mg acyl-HSL/mm^3	NA
L	Thickness of the biofilm	$L(0)=3$ μm	Assumed
z	Length, measured from substratum		
t	Time		
ζ	Rescaled length, $z=L\zeta$		
u	Material velocity		
$Y_{x/o}$	Yield of active biomass due to substrate consumption	0.583 mg VSS/mg O_2	[1,25][b]
$\hat{q}_o$	Maximum specific substrate utilization rate	8 mg O_2/(mg VSS day)	[25]
K_o	Half-maximum rate concentration for utilization of substrate	5×10^{-7} mg O_2/mm^3	[25]
$Y_{w/o}$	Yield of EPS due to substrate consumption	0.477 mg VSS/mg O_2	[1,25]
b	Endogenous decay rate coefficient	0.3/day	[25]
β_1	Basal signal production rate, associated with nutrient condition	10^{-7} mg acyl-HSL/(mg VSS day)	Estimated
β_2	Increased signal production rate in quorum sensing cells	10^{-3} mg acyl-HSL/(mg VSS day)	Estimated
β_3	Basal signal production rate, not associated with nutrient condition	10^{-4} mg acyl-HSL/(mg VSS day)	Estimated
β_4	Signal hydrolysis rate		
pH		7	NA
D_o	Substrate diffusion coefficient in the biofilm	146.88 mm^2/day	[5,34][c]
D_a	Signal diffusion coefficient in the biofilm	146.88 mm^2/day	Assumed
J_o	Substrate flux at film surface	10^3 mg O_2/(mm^2 day)	Assumed
J_a	Signal flux at film surface	10^3 mg signal/(mm^2 day)	Assumed
a_o	Signal critical threshold concentration	6.7×10^{-9} mg acyl-HSL/mm^3	Estimated
σ	Attachment/detachment rate	0 μm/day	Assumed
o_L	Substrate concentration in bulk liquid	8.3×10^{-6} mg O_2/mm^3	NA
f_D	Biodegradable fraction of active biomass	0.8	[25]
γ	mg oxygen/mg VSS	1.42 mg O_2/mg VSS	[25]

[a]Personal communication.
[b]The true yield, Y, was calculated using general parameters for an aerobic heterotroph [25]. This yield (mg VSS/mg oxygen) was divided into two fractions: cell mass ($Y_{x/o}$) and EPS ($Y_{w/o}$) [1].
[c]The diffusion coefficient for oxygen in water [1] was multiplied by 0.8 [34] to yield the diffusion coefficient for oxygen in the biofilm.

When the signal concentration (a) has reached the critical threshold (a_o), quorum sensing will be induced, and the active biomass will produce additional signal (i.e., the third term in Eq. (4)). $H(x)$, as used in Eq. (4), is the Heaviside function. It is given by:

$$H(x)=\begin{cases}1 & x\geq 0\\ 0 & \text{otherwise}\end{cases} \tag{5}$$

Therefore, when the signal concentration (a) is greater than or equal to the critical threshold (a_o), the Heaviside function will have a value of 1. This results in a nonzero value for the third term in Eq. (4), thereby yielding a much higher rate of signal production when quorum sensing has been induced.

Finally, the loss of signal is also considered. Signal could be lost due to consumption as a carbon or nitrogen source, adsorption, or hydrolysis. In this model, the loss of signal is assumed to be due to hydrolysis and to be independent of the biomass concentration. The formula used for the signal loss coefficient is:

$$\beta_4(pH)=10^{pH-7}\ln(2). \tag{6}$$

This parameter was estimated using the half-life of 3-oxohexanoyl-HSL [28], a signaling compound related to the compound of interest (3-oxododecanoyl-homoserine lactone). The net rate of signal synthesis is therefore $\mu_a f_x \rho_x - \beta_4 a$.

Dynamics

Biomass equations: Next, the kinetics is coupled to the dynamics of the one-dimensional system. We follow a derivation similar to that found in Wanner and Gujer [31]. We begin with the mass balance equation:

$$\frac{\partial}{\partial t}[Adz\rho_i f_i(t,z)] = Adz(\mu_i(t,z)\rho_i f_i(t,z)+\mu_{ij}\rho_j f_j(t,z)) + Ag_i(t,z) - A[g_i(t,z)+\frac{\partial g_i}{\partial z}(t,z)dz]. \tag{7}$$

Here, i,j can be either x or w for active biomass or inactive material, A is a representative area orthogonal to the film growth direction, and g_i is the mass flux across the surface of a small control volume of thickness dz. Eq. (7) differs from the derivation in Wanner and Gujer by the introduction of the cross-product term $\mu_{ij}\rho_j f_j$. The values of A, dz, and ρ_i are all taken to be constant, so dividing through by them yields:

$$\frac{\partial f_i}{\partial t}=\mu_i f_i+\mu_{ij}\frac{\rho_j}{\rho_i}f_j-\frac{1}{\rho_i}\frac{\partial g_i}{\partial z}. \tag{8}$$

The mass flux g_i is given by the velocity u of the mass at the point z times the mass $\rho_i f_i$, so that:

$$g_i(t,z)=u(t,z)\rho_i f_i(t,z).$$

Substituting the flux into Eq. (8) gives:

$$\frac{\partial f_i}{\partial t} = \mu_i f_i + \mu_{ij}\frac{\rho_j}{\rho_i} f_j - \frac{\partial}{\partial z}(u f_i) \tag{9}$$

The total volume contains either active biomass or inactive material, and therefore, $f_x + f_w \equiv 1$. From this, we observe:

$$\frac{\partial f_x}{\partial t} + \frac{\partial f_w}{\partial t} \equiv 0, \quad \frac{\partial}{\partial z}(u f_x) + \frac{\partial}{\partial z}(u f_w) = \frac{\partial}{\partial z}(u(f_x + f_w)) \equiv \frac{\partial u}{\partial z}.$$

Summing Eq. (9) over $i=\{x,w\}$, and noting that $\mu_{xw}=\mu_w=0$, we obtain:

$$0 = \frac{\partial f_x}{\partial t} + \frac{\partial f_w}{\partial t} = \mu_x f_x - \frac{\partial}{\partial z}(u f_x) + \mu_{wx}\frac{\rho_x}{\rho_w} f_x - \frac{\partial}{\partial z}(u f_w)$$

$$= \mu_x f_x + \mu_{wx}\frac{\rho_x}{\rho_w} f_x - \frac{\partial u}{\partial z.}$$

This equation now determines u:

$$\frac{\partial u}{\partial z} = \left(\mu_x + \frac{\rho_x}{\rho_w}\mu_{wx}\right) f_x. \tag{10}$$

Noting that the attachment surface is stationary, $u(t,0)=0$. Hence:

$$u(t,z) = \int_0^z \left(\mu_x(t,z') + \frac{\rho_x}{\rho_w}\mu_{wx}(t,z')\right) f_x(t,z')dz'. \tag{11}$$

The change in the biofilm thickness is now determined by the surface velocity $u(t,L)$ where:

$$\frac{dL}{dt} = u(t,L) + \sigma(t). \tag{12}$$

The quantity $\sigma(t)$ is the rate of surface growth due to attachment (when positive) or detachment (when negative).

Using $\mu_{xw}=0$ and $i=x$ in Eq. (9), the evolution equation for biofilm growth becomes:

$$\frac{\partial f_x}{\partial t} = \mu_x f_x - \frac{\partial}{\partial z}(u f_x), \tag{13}$$

which, together with Eq. (10), comprises the governing partial differential equations for biomass growth.

Diffusing quantities: The governing partial differential equations for the diffusing quantities, including substrate o or signal a, can be constructed in a manner similar to those of the biofilm components. The mass balance for substrate is given by:

$$\frac{\partial o}{\partial t} = \mu_o f_x \rho_x - \frac{\partial J_o}{\partial z} \tag{14}$$

where J_o is the flux. The flux is given by a combination of the underlying biomass velocity u and Fick's Law:

$$J_o = uo - D_o\frac{\partial o}{\partial z}. \tag{15}$$

Substituting this into Eq. (14) yields:

$$\frac{\partial o}{\partial t} = \mu_o f_x \rho_x - \frac{\partial}{\partial z}(uo) + D_o\frac{\partial^2 o}{\partial z^2}. \tag{16}$$

The equation for the diffusion of signal is similar, with only the additional degradation term $\beta_4 a$:

$$\frac{\partial a}{\partial t} = \mu_a f_x \rho_x - \beta_4 a - \frac{\partial}{\partial z}(ua) + D_a\frac{\partial^2 a}{\partial z^2}. \tag{17}$$

Eqs. (11)–(13), (16) and (17) represent a reaction–diffusion system of equations modeling biofilm growth coupled with signal synthesis.

Rescaling the film coordinates: To facilitate the computation, the coordinates of the system are transformed to ζ coordinates where $\zeta(t)\equiv z/L(t)$. This way, the computation in ζ coordinates is always done on the fixed interval $0\le\zeta\le 1$. If we define $\tilde{f}_x(t,z)=f_x(t,\zeta L)$, we then have:

$$\frac{\partial}{\partial z} f_x(t,z) = \frac{1}{L}\frac{\partial}{\partial \zeta}\tilde{f}_x(t,\zeta)$$

and

$$\frac{\partial}{\partial t} f_x(t,z) = \left(\frac{\partial}{\partial t} - \frac{\zeta u(t,L)}{L}\frac{\partial}{\partial \zeta}\right)\tilde{f}_x(t,\zeta). \tag{18}$$

Similar transformations for the substrate and signal equations are also employed.

Final equations: After rescaling the coordinates for the equations and boundary conditions and defining $u_L(t)=u(t,L)=\tilde{u}(t,1)$, we obtain the following model system:

$$\frac{\partial \tilde{f}_x}{\partial t} = \mu_x \tilde{f}_x - \frac{1}{L}\frac{\partial \tilde{u}}{\partial \zeta}\tilde{f}_x + \frac{1}{L}(\zeta u_L - \tilde{u})\frac{\partial \tilde{f}_x}{\partial \zeta}$$

$$\frac{\partial \tilde{o}}{\partial t} = \mu_o \tilde{f}_x \rho_x - \frac{1}{L}\frac{\partial \tilde{u}}{\partial \zeta} + \frac{1}{L}(\zeta u_L - \tilde{u})\frac{\partial \tilde{o}}{\partial \zeta} + \frac{D_o}{L^2}\frac{\partial^2 \tilde{o}}{\partial \zeta^2}$$

$$\frac{\partial \tilde{a}}{\partial t} = \mu_a \tilde{f}_x \rho_x - \beta_4 \tilde{a} - \frac{1}{L}\frac{\partial \tilde{u}}{\partial \zeta}\tilde{a} + \frac{1}{L}(\zeta u_L - \tilde{u})\frac{\partial \tilde{a}}{\partial \zeta} + \frac{D_a}{L^2}\frac{\partial^2 \tilde{a}}{\partial \zeta^2}$$

$$\frac{\partial \tilde{f}_x}{\partial t}(t,0) = \mu_x \tilde{f}_x - \left(\mu_x + \mu_{wx}\frac{\rho_w}{\rho_x}\right)\tilde{f}_x^2$$

$$\frac{\partial \tilde{f}_x}{\partial t}(t,1) = \mu_x \tilde{f}_x - \left(\mu_x + \mu_{wx}\frac{\rho_w}{\rho_x}\right)\tilde{f}_x^2$$

$$\frac{\partial \tilde{o}}{\partial \zeta}(t,0) = 0$$

$$\frac{\partial \tilde{o}}{\partial \zeta}(t,1) = L J_o(o_L - \tilde{o}(t,1))$$

$$\frac{\partial \tilde{a}}{\partial \zeta}(t,0) = 0$$

$$\frac{\partial \tilde{a}}{\partial \zeta}(t,1) = L J_a(0 - \tilde{a}(t,1))$$

$$\tilde{u}(t,\zeta) = L\int_0^\zeta \left(\mu_x(t,\zeta) + \mu_{wx}(t,\zeta)\frac{\rho_w}{\rho_x}\right)\tilde{f}_x(t,\zeta)d\zeta$$

$$\frac{dL}{dt} = \tilde{u}(t,1) + \sigma(t). \tag{19}$$

Results

We solve system (19) using a finite difference approximation method. For the chosen parameters (Table 1), the rate of substrate consumption is on a faster time scale than that for biofilm growth or signal production. Since we are primarily interested in these longer time scales, the substrate concentration is taken to be always at equilibrium. Due to significant gradients in both the signal and substrate concentrations near the biofilm surface, we must resort to a lower-order backward Euler time integration method, which avoids the nonphysical oscillations of higher order methods. Nonetheless, we have done a careful convergence study to see that the computed solution accurately reflects the true solution of system (19).

The parameters related to biofilm growth were chosen from common values in the literature, while parameters related to signal production were estimated to achieve signal concentrations consistent with those observed experimentally (Table 1). As shown in the plots, the equilibrium substrate concentration obtained by using the above-described parameters for biofilm growth resulted in oxygen penetration into the biofilm to a depth of approximately 32 μm; this is comparable to the 80-μm dissolved oxygen penetration depth measured by Xu *et al* [35] in a *P. aeruginosa* biofilm. Additionally, the model generated a 3-day biofilm thickness of approximately 200 μm (Figure 2), which is on the same order as those that have been measured experimentally [16,35]. Agreement between these computed results and experimental data supports the validity of model (19).

We next use our model to explore different rates of acyl-HSL signal production and the onset of quorum sensing in a developing biofilm. Experimental observations indicate that cells deep within a biofilm, which are presumably under nutrient-deficient conditions,

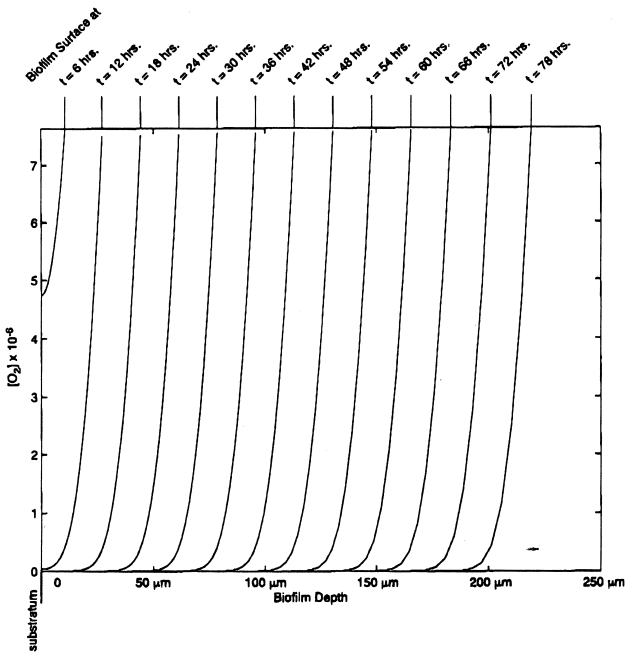

Figure 2 Plots of substrate concentration (mg/mm^3) at 6-h intervals. The substrate concentration is highest at the biofilm–liquid interface. The substratum is indicated at the bottom left. The location of the biofilm–liquid interface, at different time points, is indicated where the curve reaches the top of the graph.

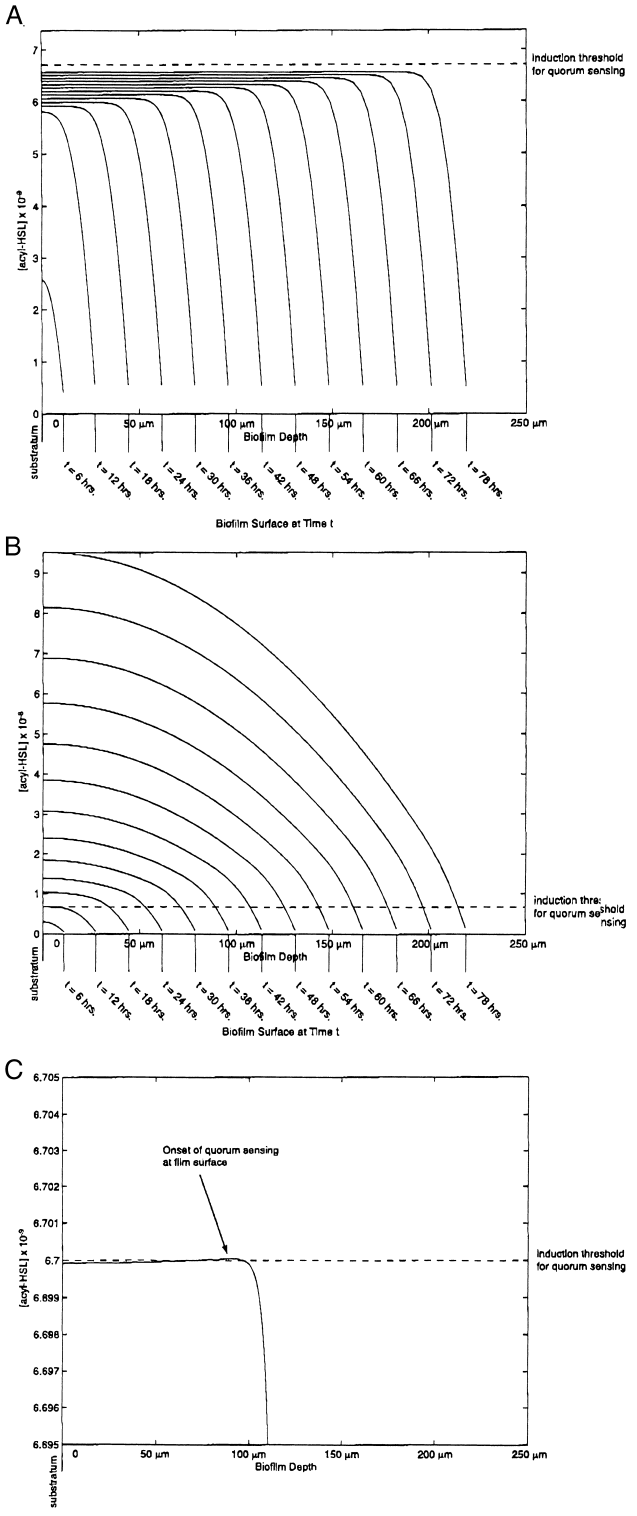

Figure 3 Plots of acyl-HSL (mg/mm^3) concentration at 6-h intervals when β_3 is 0. The concentration approaches zero at the biofilm–liquid interface. The substratum is indicated at the bottom left. The dashed line represents the inducing concentration of acyl-HSL signal. The location of the biofilm–liquid interface, at different time points, is indicated where the curve intersects the x-axis (Figure 3A and B). (A) $\beta_1 = 1.0\times10^{-2}$. (B) $\beta_1 = 1.5\times10^{-2}$. (C) $\beta_1 = 1.08\times10^{-2}$ at time 36 h.

are the first to show induction of quorum sensing [7] (MR Parsek, unpublished data). Therefore, we hypothesize that cells in nutrient-deficient parts of the biofilm may still be producing acyl-HSLs. To investigate this with our model, the parameter β_3 (basal rate of signal synthesis not associated with oxygen concentration) was set to zero, and the value of parameter β_1 (basal rate of signal synthesis associated with oxygen concentration) was varied to result in the lack of or induction of quorum sensing. Setting β_3 to zero also makes the onset of quorum sensing very sensitive to the value chosen for β_1. With a slight variation in β_1, quorum sensing may not occur (Figure 3A) or occur at the onset of biofilm growth (Figure 3B). This is because when metabolically inactive cells are not producing signal (i.e., β_3 set to zero), all signal synthesis must be in the outer layers of the biofilm where oxygen is present. For this scenario, signal synthesis must be rapid enough to generate the critical signal concentration within oxygen-containing portions of the biofilm. Interestingly, our model predicts that when β_3 is set to zero, an inducing concentration of signal is first reached in the outer layers of the biofilm (Figure 3C). This is not what we have observed experimentally, and we therefore predict that signal synthesis must also be taking place in regions of the biofilm that are oxygen-deficient. By setting $\beta_3>0$ and decreasing β_1 (Figure 4), the induction of quorum sensing is delayed, which is in agreement with experimental observations. Additionally, quorum sensing is initiated at the substratum (Figure 4), which is also in agreement with experimental observations.

The model can also be used to examine the dependency of quorum sensing on the pH in the biofilm. The signal degradation rate, $\beta_4 a$, depends on the pH according to Eq. (6). Figure 5 shows the signal concentration for the case of pH 11 (as compared to pH 7 in Figure 4) and demonstrates the sensitivity of quorum sensing induction to pH. Hence, the model is in agreement with experimental observations that quorum sensing is influenced by the pH environment [28].

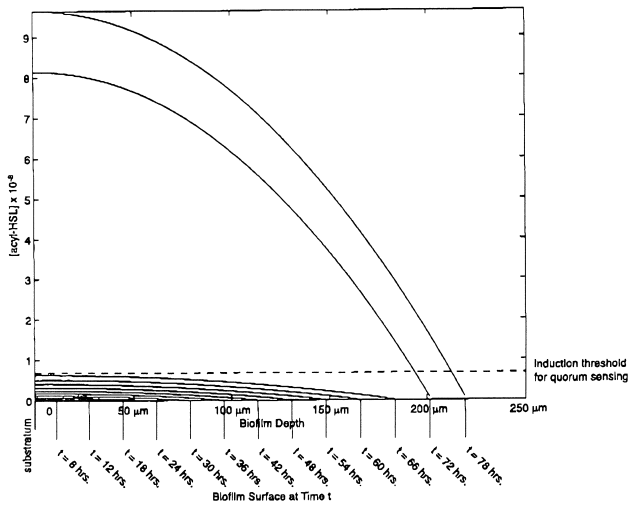

Figure 4 Plot of acyl-HSL (mg/mm^3) concentration at 6-h intervals when $\beta_3>0$. The concentration approaches zero at the biofilm–liquid interface. The substratum is indicated at the bottom left. The dashed line represents the inducing concentration of acyl-HSL signal. The location of the biofilm–liquid interface, at different time points, is indicated where the curve intersects the x-axis.

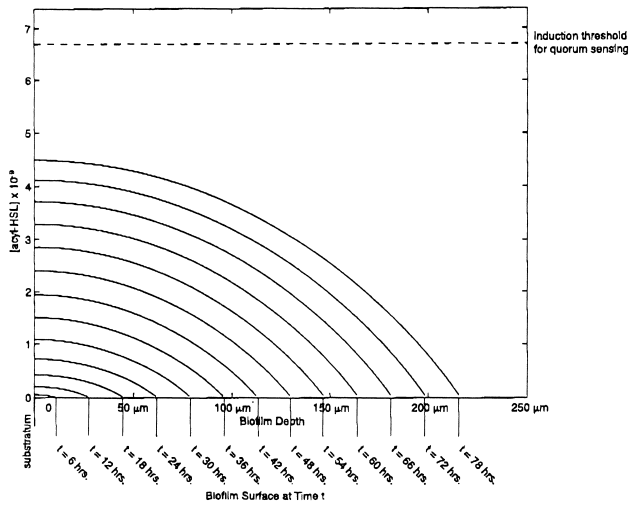

Figure 5 Plot of acyl-HSL (mg/mm^3) concentration at 6-h intervals when $\beta_3>0$. The concentration approaches zero at the biofilm–liquid interface. The substratum is indicated at the bottom left. The dashed line represents the inducing concentration of acyl-HSL signal. The location of the biofilm–liquid interface, at different time points, is indicated where the curve intersects the x-axis. Quorum sensing is not induced at pH 11.

Discussion

Quorum sensing in *P. aeruginosa* biofilms has been modeled by other groups [8,15]. Dockery and Keener [8] carefully considered acyl-HSL production and degradation at the biochemical level; however, their model *a priori* assumed a biofilm thickness and did not take into account the effects of substrate limitation to the biofilm. Nilsson *et al* [15] modeled the intracellular and extracellular concentrations of acyl-HSL in a biofilm and included the effects of acyl-HSL production, degradation, and diffusion. While this model tracked biofilm growth as a function of time, using a logistics model of population growth, it did not explicitly include the effects of biofilm decay and substrate limitation. Both groups emphasized the biochemistry of quorum sensing. The phenomenon of quorum sensing was modeled essentially as a biochemical switch; when the local concentration of the signaling compound (acyl-HSL) reached a critical threshold, its production rate increased rapidly (autocatalytically), and this in turn caused the expression of quorum sensing-regulated genes. It then becomes of interest to investigate the conditions under which the signaling compound reaches its critical concentration. In a homogeneous cell culture, this occurs at a critical population density, hence the terminology quorum sensing. In a biofilm or other spatially fixed system, the critical signal threshold can occur in regions of high local concentration of the signal compound. The concentration of the signal depends on the position in the biofilm, biofilm thickness, diffusion rates, boundary conditions at the film surface, and the kinetics of signal production.

Unlike the aforementioned models, the model developed in our research predicts acyl-HSL concentration profiles in a growing mono-species biofilm. The model predicts biofilm growth and oxygen concentration profiles that correlate well with experimental data. The model also suggests that cells in anaerobic regions of the biofilm play an important role in producing signal and predicts that a quorum may first be reached at cells near the substratum in a developing biofilm.

Our model will be further refined through additional experimentation. The model incorporates parameters describing acyl-HSL production rates, $\beta_1 - \beta_3$, which directly impact the onset of quorum sensing. However, these parameters have not been experimentally determined. Future experiments will determine acyl-HSL signal synthesis rates as a function of growth rate, substrate concentration, and quorum sensing state (i.e., on or off). Although the expression for β_4 is a plausible estimate for the base lability of signal, there could be other factors besides pH involved in signal turnover. Recent studies have shown that a number of microorganisms are capable of using acyl-HSLs as sole carbon and nitrogen sources [9,13]. Additionally, the potential for adsorption of acyl-HSLs to biofilm EPS must also be investigated. Degradative and adsorptive sinks for acyl-HSLs are a key aspect of quorum sensing in a biofilm, but they are not yet well understood.

We may also extend the model to consider other substrates in addition to dissolved oxygen. For instance, *P. aeruginosa* usually uses oxygen as an electron acceptor. However, if oxygen is limiting near the substratum, the bacteria could switch to nitrate respiration if nitrate is available. Therefore, these cells may be considered metabolically active and may be producing significant levels of signal.

Another issue to be considered is the effect of flow velocity on quorum sensing in biofilms. Biomass density (mass of cells per unit of biofilm volume) has been shown to increase when the shear stress increases [2]. By increasing the biomass density, quorum sensing could be initiated earlier during biofilm development. However, increased flow velocity could very well have the opposite effect, rapidly removing newly synthesized signal from the biofilm and into the bulk liquid.

This model, which predicts patterns of quorum sensing gene expression within a growing biofilm, has potential utility in industrial and clinical applications, such as targeting a clinical biofilm with quorum sensing inhibitors or engineering a system that relies on quorum sensing for synthesis of fermentation products. This model also helps us to analyze how the fundamental quorum sensing mechanism works in biofilm communities. Future work will use experimentation to refine important parameters and validate assumptions made in the model. Ultimately, we hope to develop a three-dimensional model, which takes into account the dynamic three-dimensional structure of biofilms and their environment.

Acknowledgements

The authors gratefully acknowledge BE Rittmann for discussions regarding microbial kinetics. This research was supported by Public Health Service grant R01 GM 67248-01 (D.L.C., B.M., M.R.P.) and NSF MCB 0133-833 (M.R.P.). M.J.K. was supported by an institutional grant, CH9810-578.

References

1 Bakke R, WG Characklis, MH Turakhia and A Yeh. 1990. Modeling a monopopulation biofilm system: *Pseudomonas aeruginosa*. In: Characklis WG and KC Marshall (Eds), Biofilms. Wiley, New York, pp. 487–520.
2 Characklis WG. 1980. Biofilm Development and Destruction. Electric Power Research Institute. Technical report: EPRI CS-1554.
3 Costerton JW, Z Lewandowski, DE Caldwell, DR Korber and HM Lappin-Scott. 1995. Microbial biofilms. *Annu Rev Microbiol* 49: 711–745.
4 Costerton JW, P Stewart and EP Greenberg. 1999. Bacterial biofilms: a common cause of persistent infections. *Science* 284: 1318–1322.
5 CRC Handbook of Chemistry and Physics, 71st edn. 1990. In: Lide DR (Ed). CRC Press, Boca Raton, FL.
6 Davies DG, MR Parsek, JP Pearson, BH Iglewski, JW Costerton and EP Greenberg. 1998. The involvement of cell-to-cell signals in the development of a bacterial biofilm. *Science* 280: 295–298.
7 De Kievit TR, R Gillis, S Marx, C Brown and BH Iglewski. 2001. Quorum-sensing genes in *Pseudomonas aeruginosa* biofilms: their role and expression patterns. *Appl Environ Microbiol* 67(4): 1865–1873.
8 Dockery JD and JP Keener. 2001. A mathematical model for quorum sensing in *Pseudomonas aeruginosa*. *Bull Math Biol* 63: 95–116.
9 Dong YH, LH Wang, JL Xu, HB Zhang, XF Zhang and LH Zhang. 2001. Quenching quorum-sensing-dependent bacterial infection by an *N*-acyl homoserine lactonase. *Nature* 411(6839): 813–817.
10 Fuqua C and EP Greenberg. 1998. Self perception in bacteria: quorum sensing with acylated homoserine lactones. *Curr Opin Microbiol* 1: 183–189.
11 Fuqua C, MR Parsek and EP Greenberg. 2001. Regulation of gene expression by cell-to-cell communication: acyl-homoserine lactone quorum sensing. *Annu Rev Genet* 35: 439–468.
12 Gambello MJ, S Kaye and BH Iglewski. 1993. LasR of *Pseudomonas aeruginosa* is a transcriptional activator of the alkaline protease gene (*apr*) and an enhancer of exotoxin A expression. *Infect Immun* 61(4): 1180–1184.
13 Leadbetter JR and EP Greenberg. 2000. Metabolism of acyl-homoserine lactone quorum-sensing signals by *Variovorax paradoxus*. *J Bacteriol* 182(24): 6921–6926.
14 More MI, LD Finger, JL Stryker, C Fuqua, A Eberhard and SC Winans. 1996. Enzymatic synthesis of a quorum-sensing autoinducer through use of defined substrates. *Science* 272(5268): 1655–1658.
15 Nilsson P, A Olofsson, M Fagerlind, T Fagerström, S Rice, S Kjelleberg and P Steinberg. 2001. Kinetics of the AHL regulatory system in a model biofilm system: how many bacteria constitute a ''quorum''? *J Mol Biol* 309(3): 631–640.
16 Okkerse WJ, SP Ottengraf and B Osinga-Kuipers. 2000. Biofilm thickness variability investigated with a laser triangulation sensor. *Biotechnol Bioeng* 70(6): 619–629.
17 Parsek MR, DL Val, BL Hanzelka, JE Cronan Jr and EP Greenberg. 1999. Acyl-homoserine lactone quorum-sensing signal generation. *Proc Natl Acad Sci USA* 96(8): 4360–4365.
18 Passador L, JM Cook, MJ Gambello, L Rust and BH Iglewski. 1993. Expression of *Pseudomonas aeruginosa* virulence genes requires cell-to-cell communication. *Science* 260(5111): 1127–1130.
19 Pearson JP, KM Gray, L Passador, KD Tucker, A Eberhard, BH Iglewski and EP Greenberg. 1994. Structure of the autoinducer required for expression of *Pseudomonas aeruginosa* virulence genes. *Proc Natl Acad Sci USA* 91(1): 197–201.
20 Pesci EC and BH Iglewski. 1997. The chain of command in *Pseudomonas* quorum sensing. *Trends Microbiol* 5(4): 132–134, discussion 134–135.
21 Pesci EC, JP Pearson, PC Seed and BH Iglewski. 1997. Regulation of *las* and *rhl* quorum sensing in *Pseudomonas aeruginosa*. *J Bacteriol* 179(10): 3127–3132.
22 Pesci EC, JB Milbank, JP Pearson, S McKnight, AS Kende, EP Greenberg and BH Iglewski. 1999. Quinolone signaling in the cell-to-cell communication system of *Pseudomonas aeruginosa*. *Proc Natl Acad Sci USA* 96(20): 11229–11234.
23 Piper KR, S Beck von Bodman and SK Farrand. 1993. Conjugation factor of *Agrobacterium tumefaciens* regulates Ti plasmid transfer by autoinduction. *Nature* 362(6419): 448–450.
24 Prigent-Combaret C, G Prensier, TT Le Thi, O Vidal, P Lejeune and C Dorel. 2000. Developmental pathway for biofilm formation in curli-producing *Escherichia coli* strains: role of flagella, curli and colanic acid. *Environ Microbiol* 2(4): 450–464.
25 Rittmann BE and P McCarty. 2001. Environmental Biotechnology. McGraw-Hill, New York.
26 Sauer K, AK Camper, GD Ehrlich, JW Costerton and DG Davies. 2002. *Pseudomonas aeruginosa* displays multiple phenotypes during development as a biofilm. *J Bacteriol* 184(4): 1140–1154.

27 Schaefer AL, DL Val, BL Hanzelka, JE Cronan Jr and EP Greenberg. 1996. Generation of cell-to-cell signals in quorum sensing: acyl homoserine lactone synthase activity of a purified *Vibrio fischeri* LuxI protein. *Proc Natl Acad Sci USA* 93(18): 9505–9509.
28 Schaefer AL, BL Hanzelka, MR Parsek and EP Greenberg. 2000. Detection, purification and structural elucidation of acylhomoserine lactone inducer of *Vibrio fischeri* luminescence and other related molecules. *Methods Enzymol* 305: 288–301.
29 Singh PK, AL Schaefer, MR Parsek, TO Moninger, MJ Welsh and EP Greenberg. 2000. Quorum-sensing signals indicate that cystic fibrosis lungs are infected with bacterial biofilms. *Nature* 407(6805): 762–764.
30 Stewart PS and JW Costerton. 2001. Antibiotic resistance of bacteria in biofilms. *Lancet* 358(9276): 135–138.
31 Wanner O and W Gujer. 1986. A multispecies biofilm model. *Biotechnol Bioeng* 28: 314–328.
32 Watnick P and R Kolter. 2000. Biofilm, city of microbes. *J Bacteriol* 182(10): 2675–2679.
33 Whiteley M, MG Bangera, RE Bumgarner, MR Parsek, GM Teitzel, S Lory and EP Greenberg. 2001. Gene expression in *Pseudomonas aeruginosa* biofilms. *Nature* 413(6858): 860–864.
34 Williamson KJ and PL McCarty. 1976. Verification studies of the biofilm model for bacterial substrate utilization. *J Water Pollut Control Fed* 48: 281–289.
35 Xu KD, PS Stewart, F Xia, CT Huang and GA McFeters. 1998. Spatial physiological heterogeneity in *Pseudomonas aeruginosa* biofilm is determined by oxygen availability. *Appl Environ Microbiol* 64: 4035–4039.